Application of a Point-Matching MoM Reduced Scheme to Scattering from Finite Cylinders

Antonis G. Papagiannakis, *Member, IEEE*

***Abstract*— One of the most common methods for the solution of three-dimensional (3-D) scattering problems is the electric-field volume integral equation numerically solved by the application of the method of moments (MoM)—usually the point-matching version. Although simple to formulate, it shows inherent difficulty and complexity because of the 3-D integrals appearing in the interaction matrix elements and of the singularity of the dyadic Green's function (DGF) present in the computation of the self-cell elements. In this paper, a transformation method is presented, which in the case of the point-matching MoM, both reduces the 3-D integrals to two-dimensional (2-D) ones, and also eliminates the need of separate treatment of the singularity while maintaining the same degree of approximation. Comparison to published results is made for the case of scattering by a finite dielectric cylinder. Further examples are presented for scattering by layered dielectric cylinders and lossy cylindrical shells excited by uniform plane waves.**

***Index Terms*— Cylinders, dielectric bodies, electromagnetic scattering, moment methods.**

I. Introduction

THE PROBLEM of scattering of an incident field by dielectric (perfect or lossy) scatterers is a subject of great interest in the study of phenomena such as propagation through rain, snow or forests, radiation of antennas in the presence of inhomogeneities and obstacles, power absorption by biological tissues for medical diagnosis purposes or for hyperthermia in cancer therapy, coupling to airborne bodies possibly with dielectric-filled apertures, and many other manifestations of electromagnetic-field interaction with material bodies. The methods used to attack these problems present a great variety being analytical, semianalytical, or numerical. However, the complexity of such three-dimensional (3-D) problems almost inevitably leads to the use of numerical methods for the computation of the internal field as well as the far field characteristics [1], [2]. Whereas asymptotic methods based on the Rayleigh–Born approximation are suitable for the low-frequency regime, and asymptotic techniques such as the Wentzel–Kramer–Brillouin (WKB) method and the geometrical theory of diffraction are suitable in the high-frequency regime, the so-called resonance region, where the objects are of the order of a wavelength, necessitates an exact solution of Maxwell's equations.

Manuscript received February 14, 1996; revised May 19, 1997.

The author is with the Telecommunications Division, Electrical and Computer Engineering Department, Aristotle University of Thessaloniki, GR-54 006 Thessaloniki, Greece.

Publisher Item Identifier S 0018-9480(97)06057-2.

A method commonly used in this region is the use of the equivalent polarization currents and the formulation of an integral equation for the field inside the scatterer [3], [4]. The integral equation can subsequently be transformed to an algebraic system and solved numerically by the application of the method-of-moments (MoM) technique [1]–[6]. The most preferably used version of the MoM is the point-matching one. It is simple to formulate and apply, can treat homogeneous as well as inhomogeneous problems, gives both the internal and the external field, and yields sufficiently accurate results, especially for far-field and other averaged characteristics.

One of the most serious drawbacks and difficulties in the application of the point-matching MoM is, besides the large arrays obtained, the 3-D volume integrals that have to be numerically computed for the evaluation of the cell-interaction array elements. These 3-D integrals are time-consuming and difficult to compute, especially for arbitrary cell shapes, and they usually require additional approximations. In addition, special care must be taken and further approximations must be made in the evaluation of the diagonal elements, which represent the self-cell interaction and contain the singularity of the Green's function in the self dyad [1]–[8].

The effort to reduce the burden of computation of the interaction array elements and to effectively treat the self-cell singularity is evident in works using the MoM [11], [14]–[26]. The numerical treatment of the singularity can be made by analytically transforming the singular integral, confining the source point within a cell of arbitrary shape and size, and numerically evaluating the integrals [22]. However, in this case the number of volume integrals per cell increases to two or three, while the nearly singular behavior of the integrals is not avoided in the case of small self-cell volume. When the source distribution is uniform or linear, Gauss' integral theorem has been used to reduce the dimension of the singular integral, mainly in the static case [23], but the cell shape can only be polygonal with straight edges or polyhedral with planar sides. Also, integration of the Green's function derivatives is not considered. The use of linear-shape functions extends the method and integration of the gradient of the scalar Green's function is achieved for planar triangular cells [25], [26]. The use of FEM-type elements (linear or parametric) for describing the scatterer volume allows one to reduce the singular volume integral to a surface one and also gives greater flexibility in representing complex shapes [24], [25], but the number of volume integrations per cell is again increased to three and point matching is used in the examples presented.

In the present paper, a transformation method is presented, which in the case of the point-matching MoM, reduces the 3-D volume integral in the computation of the cell-interaction array elements to a two-dimensional (2-D) one over the boundary surface of the cell. In this way, the complexity and the time needed in order to evaluate these elements is also reduced and at the same time, the need for separate treatment of the self-dyad singularity is eliminated. While the point-matching MoM assumes piecewise uniform sources, the general form of the surface integral allows accurate representation of the scatterer shape and no volume rescaling is needed. It is also proven that the degree of approximation introduced by the point-matching MoM is maintained. The verification of the method and the validation of the computer code written is made by solving the problem of scattering by a finite dielectric cylinder with a uniform plane-wave excitation. The cylindrical structures, more than the also widely used spherical ones, offer an effective and efficient model for the simulation of many practical objects such as trees, the human body, airplanes, missiles, and antennas [9]–[21]. The variety of methods introduced in analyzing their behavior reflects both the complexity and the importance of the problem of the 3-D scatterer in general and the cylindrical one in particular. The verification of the scheme presented in this paper is made by comparison to published results. Further examples for the scattering of a uniform plane wave by finite cylindrical structures, namely a coated dielectric cylinder, a hollow layered dielectric cylinder, and a lossy cylinder with dielectric coating are presented.

II. Mathematical Treatment

Consider a finite 3-D scatterer of relative complex permittivity ε_r excited by an incident field $\vec{E}^{\text{inc}}$. When the scatterer volume is replaced by its equivalent dielectric polarization currents, the following volume integral equation results for the total electric field $\vec{E}(\vec{r})$ in the volume V of the scatterer [3], [4], [7]:

$$\vec{E}^{\text{inc}}(\vec{r}) = \vec{E}(\vec{r}) - k_0^2 \int_V \overleftrightarrow{G}_0(\vec{r},\vec{r}') \cdot (\varepsilon_r - 1)\vec{E}(\vec{r}')\, dv' \quad (1)$$

where $\overleftrightarrow{G}_0(\vec{r},\vec{r}')$ is the free-space dyadic Green's function (DGF) [7, eq. (4.44)], k_0 is the free-space wavenumber, and $\vec{r}$ is located within V. In order to solve (1) by the point-matching MoM the volume of the scatterer is divided into a number N of cells. Assuming that the number of the cells is large enough, such that the field and the permittivity within each cell can be considered constant, (1) is applied to the centers of all cells and the integral equation is transformed to an algebraic system [1], [2], [5]

$$[\overleftrightarrow{g}_{c_2c_1}] \cdot \{(\varepsilon_{c_1} - 1)\vec{E}_{c_1}\} = \{\vec{E}^{\text{inc}}_{c_2}\}. \quad (2)$$

The solution of the system in (2) yields the normalized dielectric polarization vector $[(\varepsilon_{c_1} - 1)\vec{E}_{c_1}]$ in each cell (ε_{c_1} is the relative complex permittivity of the cell c_1). Each dyadic element $\overleftrightarrow{g}_{c_2c_1}$ of the cell interaction matrix in (2) represents the contribution of the field in cell c_1 to the field in cell c_2 and it is given by the relation

$$\overleftrightarrow{g}_{c_2c_1} = \overleftrightarrow{I}\frac{\delta^{c_2c_1}}{\varepsilon_{c_1} - 1} - k_0^2 \int_{V_{c_1}} \overleftrightarrow{G}_0(\vec{r}_{c_2},\vec{r}')\, dv' \quad (3)$$

where $\overleftrightarrow{I}$ is the unit dyadic (idemfactor), $\delta^{c_2c_1}$ is Kronecker's delta, $\vec{r}_{c_2}$ points at the center of cell c_2, and V_{c_1} is the volume of cell c_1. The numerical evaluation of the dyadic elements $\overleftrightarrow{g}_{c_2c_1}$ is the most difficult and time-consuming part in the application of the MoM, mainly because of the following two reasons: a 3-D volume integral has to be computed numerically for each component of the $\overleftrightarrow{g}_{c_2c_1}$ dyadic, and in the case of the self-cell interaction, the Green's function in the integrand of (3) becomes singular and special treatment or approximation has to be used for the numerical evaluation of the integrals.

It would be very helpful if these problems could be alleviated while the degree of approximation introduced by the point-matching MoM is maintained. This can be done by transforming the volume integral in (3) into a surface one. For such a reduction, the free-space DGF in the integrand of (3) is substituted from the defining vector Helmholtz equation [7, eq. (4.37)]

$$\nabla' \times \nabla' \times \overleftrightarrow{G}_0(\vec{r}',\vec{r}_{c_2}) - k_0^2\overleftrightarrow{G}_0(\vec{r}',\vec{r}_{c_2}) = \overleftrightarrow{I}\delta(\vec{r}' - \vec{r}_{c_2}) \quad (4)$$

where ∇' means differentiation with respect to the primed variables. Two integrals are thus obtained. The first one is evaluated using the sifting property of the Dirac delta function. The second one is transformed to a surface integral by using the dyadic Stokes theorem [derived from [7, eq. (A.44)] for $\vec{P} = \text{const.}$). The application of the symmetrical properties of the free-space DGF obeying the radiation condition at infinity [7, Table IV-1] gives the final result

$$\begin{aligned} &-k_0^2 \int_{V_{c_1}} \overleftrightarrow{G}_0(\vec{r}_{c_2},\vec{r}')\, dv' \\ &\quad = \overleftrightarrow{I}\delta^{c_1c_2} + \oint_{S_{c_1}} [(\nabla \times \overleftrightarrow{G}_0(\vec{r}_{c_2},\vec{r}')) \times \hat{n}]\, ds' \end{aligned} \quad (5)$$

where S_{c_1} is the boundary surface of volume V_{c_1} and $\hat{n}$ is its outward-unit normal vector.

Although (5) has been formally obtained from (4), the proof is correct if the DGF is considered in the distributional sense. This consideration especially covers the self-dyad case (i.e., when $c_1 = c_2$) when the DGF singularity is contained in the integration volume. Otherwise the proof in this case can be made by isolating the singularity in a shrinking volume, as in [8]. Equation (5) can be considered as describing an equivalent problem, where electric volume sources have been replaced by magnetic surface ones. However, since (5) is obtained with mere algebraic manipulation, this equivalence is not clear enough. A stricter proof (which also clarifies the equivalent problems involved and permits the investigation of the approximation errors) can be made with the use of the second Green's theorem, always in the sense of distributions.

The field scattered by cell c is given by

$$\vec{E}^{\text{scatt}}_c(\vec{r}) = k_0^2 \int_{V_c} \overleftrightarrow{G}_0(\vec{r},\vec{r}') \cdot (\varepsilon_c - 1)\vec{E}_c(\vec{r}')\, dv'. \quad (6)$$

The field $\vec{E}_c$ inside the cell can be written as the sum of a constant part $\vec{C}$ and a varying part $\vec{e}$ as follows:

$$\vec{E}_c(\vec{r}') = \vec{C} + \vec{e}(\vec{r}'). \tag{7}$$

The parts of the $\vec{E}_c^{\text{scatt}}$ field due to $\vec{C}$ and $\vec{e}$ are both given by expressions similar to (6).

The assumption that the field and the permittivity within cell c are constant yields

$$\vec{E}_c^{\text{scatt}}(\vec{r}) \cong k_0^2 \int_{V_c} \overleftrightarrow{G}_0(\vec{r},\vec{r}')\, dv' \cdot [(\varepsilon_c - 1)\vec{C}]. \tag{8}$$

In view of the limiting procedure (number of cells tends to infinity, cell volume tends to zero) used in the formulation of the MoM, (8) means that

$$\left| k_0^2 \int_{V_c} \overleftrightarrow{G}_0(\vec{r},\vec{r}') \cdot (\varepsilon_c - 1)\vec{e}(\vec{r}')\, dv' \right| \ll \left| k_0^2 \int_{V_c} \overleftrightarrow{G}_0(\vec{r},\vec{r}')\, dv' \cdot [(\varepsilon_c - 1)\vec{C}] \right| \tag{9}$$

which, assuming that ε_c is constant, defines the approximation error R for the point matching MoM as

$$R = \left| k_0^2 \int_{V_c} \overleftrightarrow{G}_0(\vec{r},\vec{r}') \cdot (\varepsilon_c - 1)\vec{e}(\vec{r}')\, dv' \right| \cong 0 \tag{10}$$

as done in a simple trapezoidal quadrature rule.

Replacing $(\vec{r}', \vec{r}_{c_2})$ by $(\vec{r}, \vec{r}')$ in (4) and using the resulting equation in the second Green's theorem [7, eq. (A.45)] as applied to any arbitrary vector $\vec{J}(\vec{r}')$ and the free-space DGF $\overleftrightarrow{G}_0(\vec{r},\vec{r}')$ yields the identity

$$\begin{aligned} -k_0^2 &\int_V \overleftrightarrow{G}_0(\vec{r},\vec{r}') \cdot \vec{J}(\vec{r}')\, dv' \\ &\equiv \vec{J}(\vec{r}) U_V(\vec{r}) \\ &\quad - \int_V \overleftrightarrow{G}_0(\vec{r},\vec{r}') \cdot [\nabla' \times \nabla' \times \vec{J}(\vec{r}')]\, dv' \\ &\quad + \oint_S [(\nabla \times \overleftrightarrow{G}_0(\vec{r},\vec{r}')) \times \hat{n} \cdot \vec{J}(\vec{r}') \\ &\quad + \overleftrightarrow{G}_0(\vec{r},\vec{r}') \cdot (\hat{n} \times \nabla' \times \vec{J}(\vec{r}'))]\, ds' \end{aligned} \tag{11}$$

where $U_V(\vec{r})$ is the step function of volume V with the value of one within V and zero outside V. The values of the vectors and dyads in the surface integral of (11) are considered in the sense of the limit with $\vec{r}'$ tending to S from within the volume V. If $\vec{J}(\vec{r})$ describes an electric-current source distribution [7, eq. (4.146)], (11) establishes an equivalent problem, where the initial electric volume sources are replaced by equivalent electric volume, electric surface, and magnetic surface sources.

Replacing $\vec{J}(\vec{r})$ in (11) by the constant vector $\vec{C}$, (5) is actually proved, and in view of (8), the field scattered by cell c is given by

$$\vec{E}_c^{\text{scatt}}(\vec{r}) \cong -\left[\overleftrightarrow{I} U_{V_c}(\vec{r}) + \oint_{S_c} [(\nabla \times \overleftrightarrow{G}_0(\vec{r},\vec{r}')) \times \hat{n}]\, ds' \right] \cdot [(\varepsilon_c - 1)\vec{C}]. \tag{12}$$

Thus, the constant volume (polarization) current sources have been clearly replaced by equivalent surface magnetic-current sources. The whole process of obtaining (12) describes a sequence of equivalent problems, where the dielectric volume is replaced by its equivalent polarization currents, which are in turn approximated by constant volume electric currents, which are finally replaced by equivalent surface magnetic currents.

Consider now that within V_c, the Helmholtz equation for $\vec{E}_c(\vec{r}')$ gives

$$\nabla' \times \nabla' \times \vec{e}(\vec{r}') = \nabla' \times \nabla' \times \vec{E}_c(\vec{r}') = k_0^2 \varepsilon_c \vec{E}_c(\vec{r}'). \tag{13}$$

In view of (6) and for constant cell permittivity, we obtain

$$(\varepsilon_c - 1) \int_{V_c} \overleftrightarrow{G}_0(\vec{r},\vec{r}') \cdot \nabla' \times \nabla' \times \vec{e}(\vec{r}')\, dv' = \varepsilon_c \vec{E}_c^{\text{scatt}}(\vec{r}). \tag{14}$$

Applying the identity of (11) to the varying part $\vec{e}$ of the scattered field, and in view of (10), it is proved that (8) and (12) produce the same approximation error R. Note that although the volume distribution of $\vec{e}$ gives a negligible approximation error R, the $\nabla' \times \nabla' \times \vec{e}(\vec{r}')$ integration term in (11) gives a substantial field, as is manifested by (14). This field is made negligible only by the counteraction of the field produced by the surface values of $\vec{e}$. This remark should be kept in mind if by substituting (7) into (11) we had chosen to first replace the polarization currents by volume electric, surface electric, and surface magnetic currents, and then neglect the contribution of $\vec{e}$. False use of (13) or (14) in (11) before neglecting the contribution of $\vec{e}$ could lead to erroneous results.

By now substituting (5) into (3), the dyadic element $\overleftrightarrow{g}_{c_2c_1}$ of the cell interaction matrix is transformed to

$$\overleftrightarrow{g}_{c_2c_1} = \overleftrightarrow{I} \frac{\varepsilon_{c_1}}{\varepsilon_{c_1} - 1} \delta^{c_2c_1} + \oint_{S_{c_1}} [(\nabla \times \overleftrightarrow{G}_0(\vec{r}_{c_2},\vec{r}') \times \hat{n}]\, ds'. \tag{15}$$

The curl of the free-space DGF vectorially postmultiplied by $\hat{n}$ is evaluated as

$$[\nabla \times \overleftrightarrow{G}_0(\vec{r}_{c_2},\vec{r}')] \times \hat{n} = \frac{1}{R} \frac{dG_0(\vec{r}_{c_2},\vec{r}')}{dR} [\hat{n}\vec{R} - (\hat{n} \cdot \vec{R})\overleftrightarrow{I}] \tag{16}$$

where

$$\begin{aligned} \vec{R} &= \vec{r}_{c_2} - \vec{r}' \\ \frac{dG_0(\vec{r}_{c_2},\vec{r}')}{dR} &= -\left(jk_0 + \frac{1}{R} \right) \frac{e^{-jk_0R}}{4\pi R} \end{aligned} \tag{17}$$

and the $\overleftrightarrow{g}_{c_2c_1}$ dyad is finally given by

$$\begin{aligned} \overleftrightarrow{g}_{c_2c_1} &= \overleftrightarrow{I} \frac{\varepsilon_{c_1}}{\varepsilon_{c_1} - 1} \delta^{c_2c_1} + \overleftrightarrow{L} - \overleftrightarrow{I}\, \text{trace}\{\overleftrightarrow{L}\} \\ \overleftrightarrow{L} &= \oint_{S_{c_1}} \frac{1}{R} \frac{dG_0(\vec{r}_{c_2},\vec{r}')}{dR} \hat{n}\vec{R}\, ds'. \end{aligned} \tag{18}$$

Instead of using the dyadic notation, (18) and (5) can be alternatively derived by using the scalar free-space Green's function and the mixed potential formulation for the electric field [27]. By (18), the evaluation of the interaction matrix elements has in all cases been reduced to the evaluation of a 2-D integral instead of a 3-D one, presenting no singularity in the integrand. Nine scalar-surface integrals are nominally present for each face of the surface S_{c_1} in the dyadic integral $\overleftrightarrow{L}$ of (18). They can, however, be reduced to a number of one

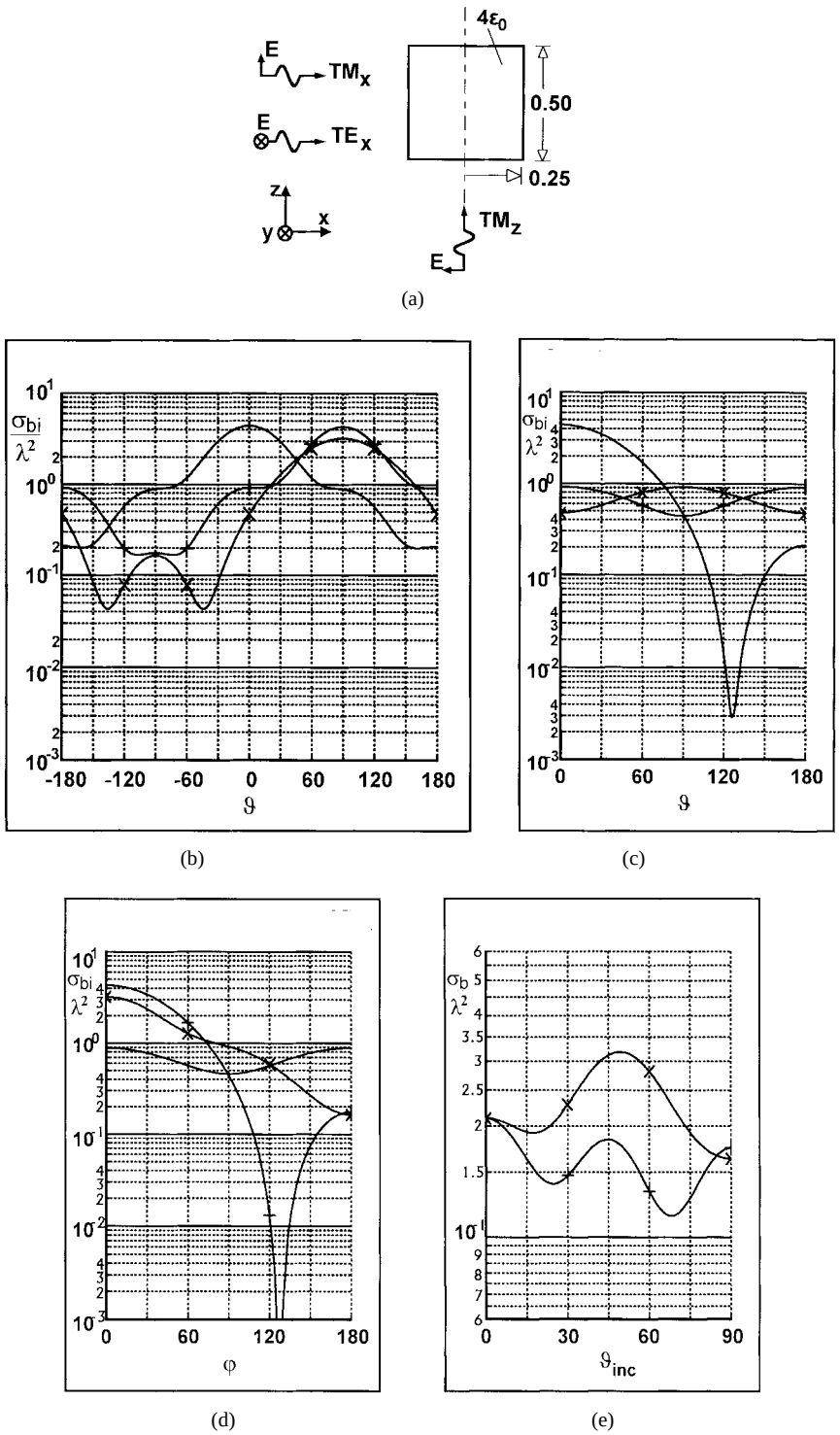

Fig. 1. Homogeneous dielectric cylinder. (a) Geometry. (b) Normalized BCS on incidence plane, (c) on yOz plane, and (d) on equatorial plane. (e) Normalized radar cross section versus ϑ_{inc}.(+ : TM_x, × : TE_x —: TM_z).

to six, depending on the shape and orientation of the surface if the integration is performed in a local coordinate system and symmetry is exploited. In an alternative formulation tested, where the cells are replaced with equivalent identical cylindrical cells of equal base area, the number of scalar integrations is further reduced with the cost of extra, yet negligible, approximation error.

The method used to reduce the 3-D integrals to 2-D ones can also be used for the computation of the scattering amplitude $\vec{f}(\hat{r})$. This is defined for any cell by [4, eq. (10-2)]

$$\vec{E}_c^{\mathrm{scatt}}(\vec{r}) = \frac{e^{-jk_0 r}}{r}\vec{f}_c(\hat{r}). \tag{19}$$

If $\vec{r}_c$ is the coordinate vector of the center of cell c and $\hat{r}$ is the direction of observation, the scattering amplitude is obtained

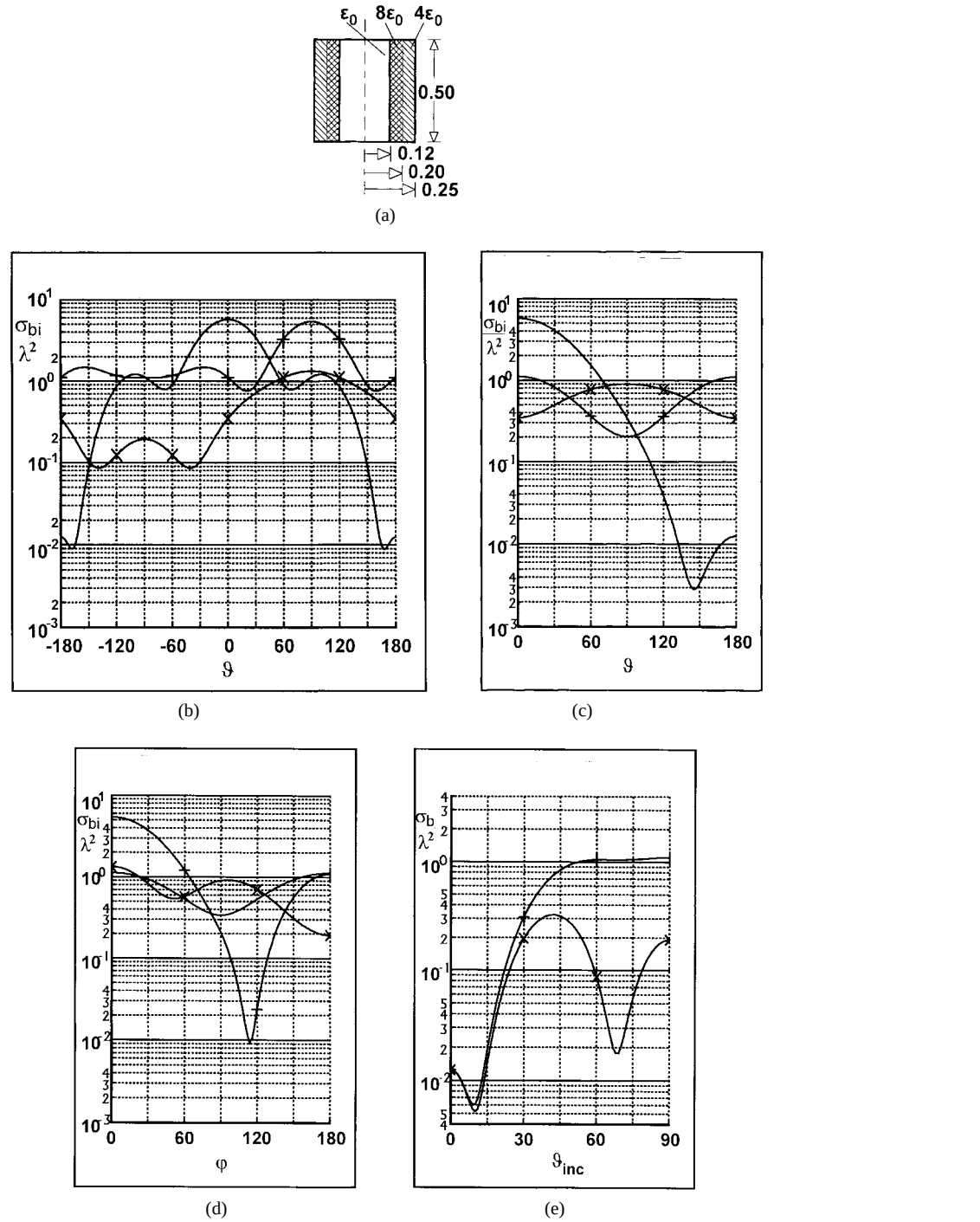

Fig. 2. Hollow layered dielectric cylinder. (a) Geometry. (b) Normalized BCS on incidence plane, (c) on yOz plane, and (d) on equatorial plane. (e) Normalized radar cross section versus ϑ_{inc}.$(+ : \mathrm{TM}_x, \times : \mathrm{TE}_x$ —: $\mathrm{TM}_z)$.

by substituting (16) and (17) into (12) with $S_{c_1} = S_c, \vec{r}_{c_2} = \vec{r}$ and $|\vec{r}| \to \infty$. It follows that

$$\vec{f}_c(\vec{r}) = -j\frac{k_0}{4\pi}e^{+jk_0\vec{r}_c\cdot\hat{r}}[(\vec{L}\cdot\hat{r})\overleftrightarrow{I} - \vec{L}\hat{r}]\cdot[(\varepsilon_c - 1)\vec{E}_c]$$
$$\vec{L} = \oint_{S_c} e^{+jk_0\vec{R}'\cdot\hat{r}}\hat{n}\, ds' \tag{20}$$

where $\vec{R}'$ is the vector from the cell center to the integration point on the cell surface. By transforming the surface integral to a volume one through the use of the Gauss gradient theorem [7, eq. (A.33)], it is proved that $\vec{L}$ is parallel to $\hat{r}$ so that

$$\vec{L} = (\vec{L}\cdot\hat{r})\hat{r} = L\hat{r}. \tag{21}$$

Hence, the scattering amplitude in (20) can be rewritten as

$$\vec{f}_c(\hat{r}) = \overleftrightarrow{I}_\perp \cdot \vec{F}_c(\hat{r})$$
$$\vec{F}_c(\hat{r}) = -j\frac{k_0}{4\pi}e^{+jk_0\vec{r}_c\cdot\hat{r}}L[(\varepsilon_c - 1)\vec{E}_c]$$
$$L = \oint_{S_c} e^{+jk_0\vec{R}'\cdot\hat{r}}\hat{n}\cdot\hat{r}\, ds'$$
$$\overleftrightarrow{I}_\perp = \hat{\vartheta}\hat{\vartheta} + \hat{\varphi}\hat{\varphi} = \overleftrightarrow{I} - \hat{r}\hat{r}. \tag{22}$$

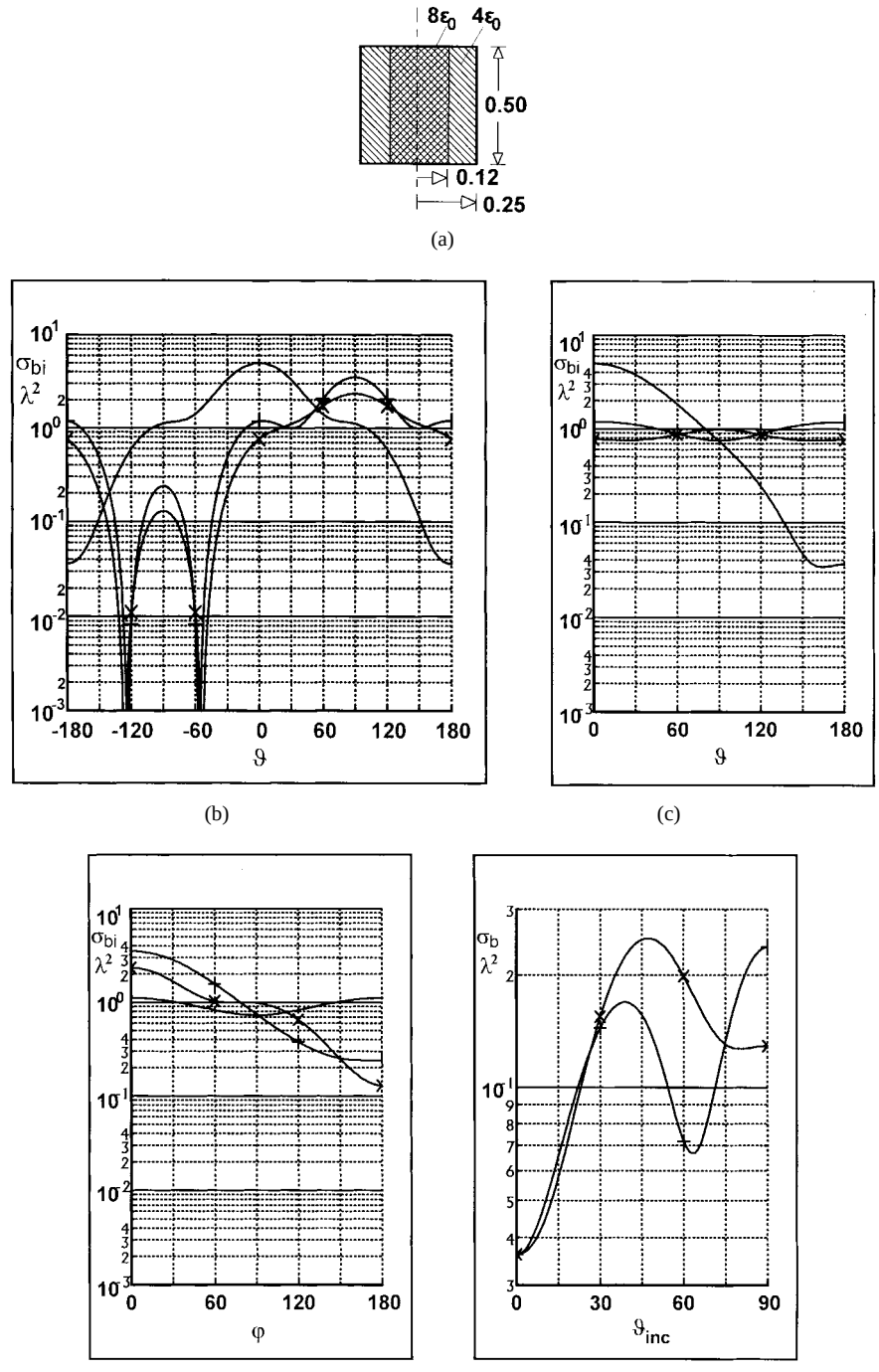

Fig. 3. Coated dielectric cylinder. (a) Geometry. (b) Normalized BCS on incidence plane, (c) on yOz plane, and (d) on equatorial plane. (d) Normalized radar cross section versus ϑ_{inc}. (+ : TM_x, × : TE_x —: TM_z).

For a total number N of cells, the scattering amplitude is given by

$$\vec{f}(\vartheta,\varphi)=\vec{f}(\hat{r})=\overleftrightarrow{I}_{\perp}\cdot\sum_{c=1}^{N}\vec{F}_c(\hat{r}) \tag{23}$$

and the bistatic cross section (BCS) normalized by the square of the free-space wavelength and for $|\vec{E}^{\mathrm{inc}}|=1$ is given by

$$\frac{\sigma_{bi}(\hat{r})}{\lambda_0^2}=\frac{4\pi}{\lambda_0^2}|\vec{f}(\hat{r})|^2=\frac{4\pi}{\lambda_0^2}\vec{f}(\hat{r})\cdot\vec{f}^{*}(\hat{r}). \tag{24}$$

Thus, the scattering amplitude necessitates the numerical evaluation of only one scalar surface integral for each cell.

III. Numerical Application

For the verification of the method and the validation of the computer code, the problem of a dielectric cylinder $(\varepsilon_r=4)$ with base radius $R=0.25\lambda_0$ and height $h=0.5\lambda_0$, excited by a uniform plane wave is used. Three cases of incidence are considered: TM_x, TE_x, TM_z, the notation describing plane waves with the specified field vector transverse to the

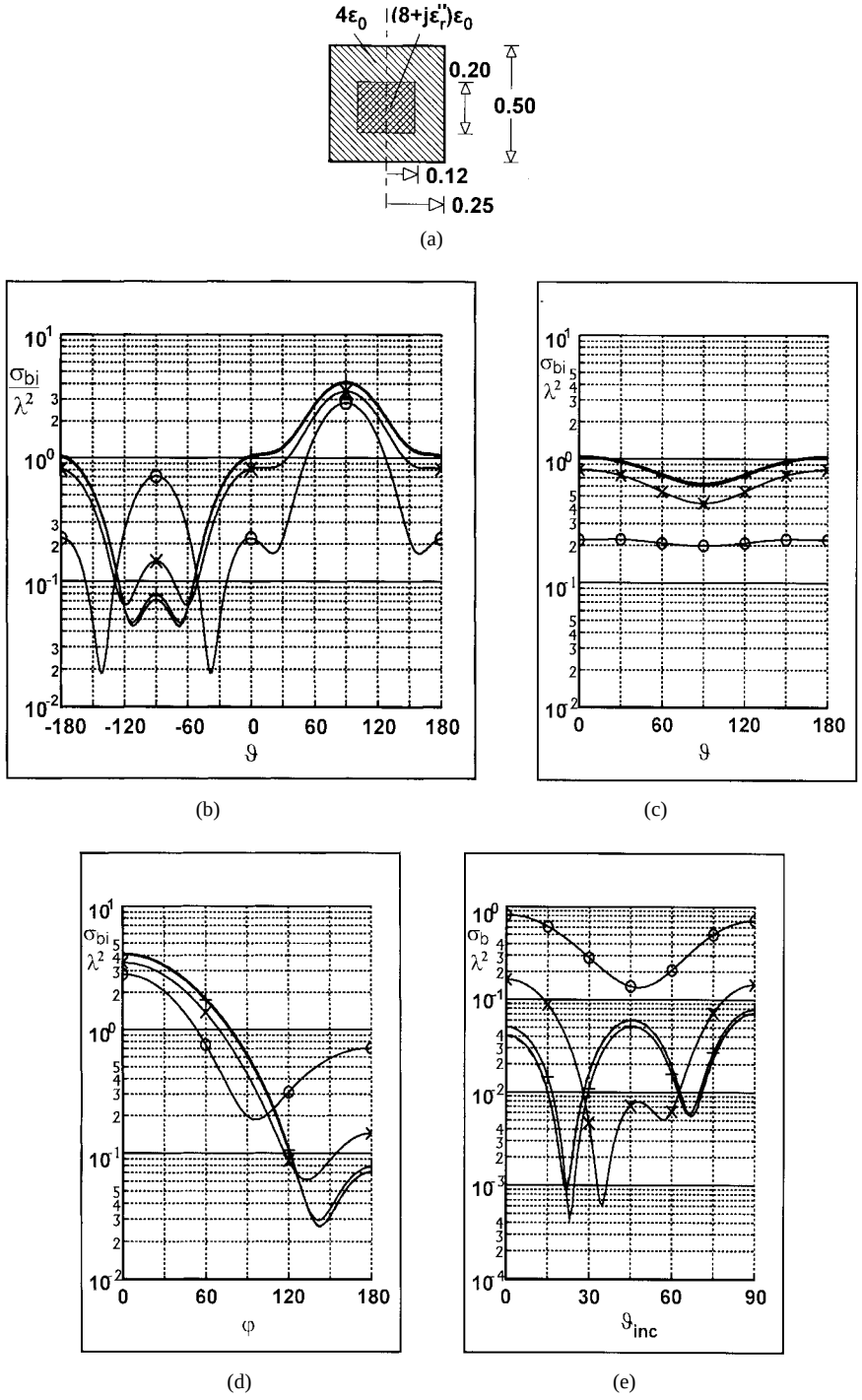

Fig. 4. Lossy cylinder with dielectric coating, TM_x incidence. (a) Geometry. (b) Normalized BCS on incidence plane, (c) on yOz plane, and (d) on equatorial plane. (e) Normalized radar cross section versus ϑ_{inc}.(ε_r'': (solid line): 0, (dashed line): $0.03, + : 0.3, \times : 3, \circ : 30$).

incidence plane xOz and propagating in the positive direction of the axis denoted by the subscript [Fig. 1(a)]. For the application of the MoM, the base of the cylinder is divided into a number of concentric rings and each ring into a number of sectors, in such a way that the base is eventually subdivided into N_b equal areas. The height of the cylinder is divided into N_h disks of equal height. Thus, a total number of $N_b \times N_h$ cells of equal volume is obtained and the cell boundary surfaces follow the reference surfaces of the cylindrical coordinate system local to the cylinder. The convergence check showed that a number of $N_b \times N_h = 52 \times 10 = 520$ cells provided the best compromise between the time and memory needed and the accuracy obtained. The computed results for the TM_z case [solid line in Fig. 1(b) and (c)] show very good agreement with previously published ones [9]. Typical run time for filling the complex and fully populated interaction matrix is about 15 min, yielding an average time of 0.37 ms per element or 3.3 ms per cell; actual time is a little more, since the program exploits the symmetry wherever possible. Computations have been implemented on an HP730 Apollo workstation using

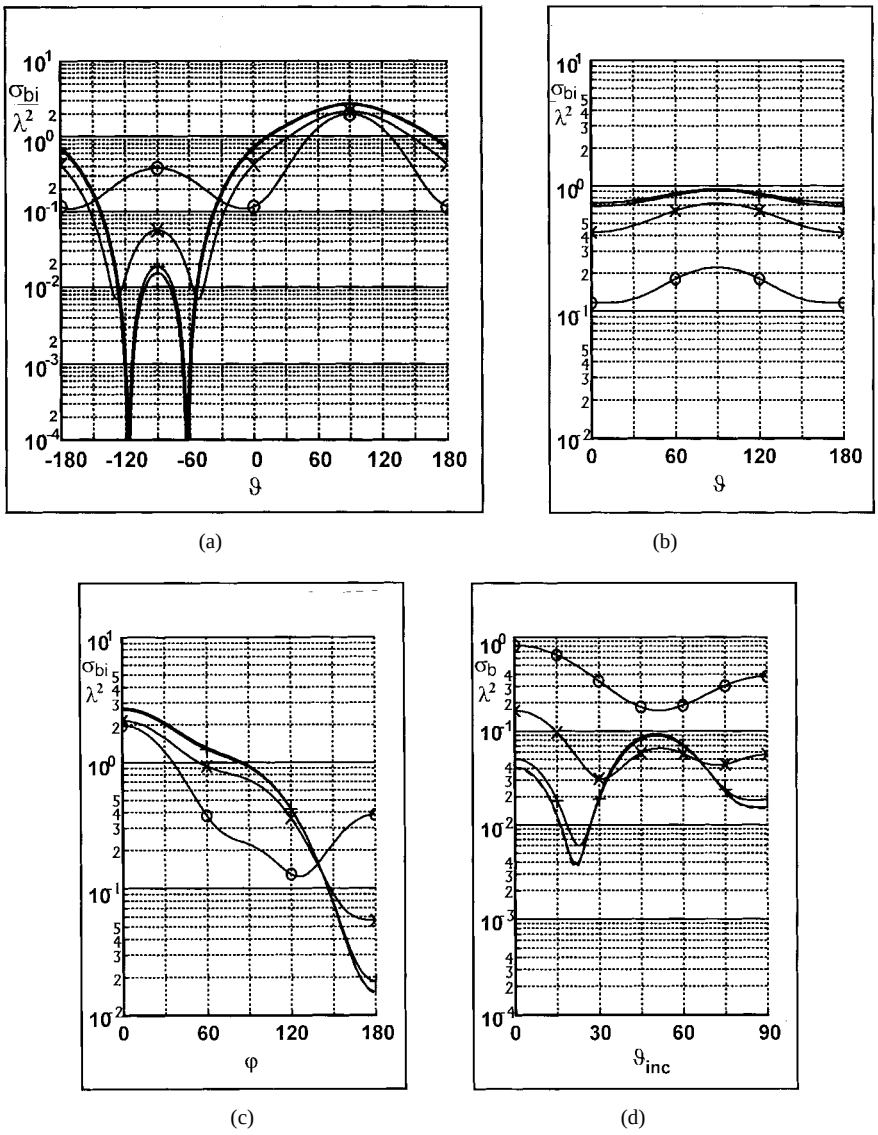

Fig. 5. Lossy cylinder with dielectric coating, TE_x incidence. (a) Normalized BCS on incidence plane, (b) on yOz plane, and (c) on equatorial plane. (d) Normalized radar cross section versus ϑ_{inc}.(ε_r'': (solide line): 0, (dashed line): $0.03, + : 0.3, \times : 3, \circ : 30$).

FORTRAN77 and a simple Simpson 1/3 quadrature rule for the evaluation of the integrals.

The normalized BCS on the three Cartesian coordinate planes is plotted in Fig. 1(b)–(d), respectively. The existing symmetry with respect to the xOz incidence plane has been exploited in drawing the figures. From the plots it can be seen that the homogeneous cylinder shows directivity to the incidence direction with a small backscattering lobe. The radar cross section (RCS) versus ϑ_{inc} [Fig. 1(e)] has its maximum at about 50° for TE incidence, whereas for TM incidence presents three local maxima at angles 0, 45, and 90°.

The second example treated is a hollow layered dielectric cylinder [Fig. 2(a)]. From the BCS plots [Fig. 2(b)–(d)] it can be seen that although the directivity is increased compared to the homogeneous cylinder case, the curves are smoother and a stronger backscattering exists for the TM case, whereas the TE_x scattering is weaker. It is also worth noting that the TM (RCS) [Fig. 2(e)] is almost constant for large angles of incidence, as we tend to the broadside incidence case.

In contrast to the previous example, the coated dielectric cylinder [Fig. 3(a)] presents high directivity for the TM_z case and a reduced and more uniform one for the TM_x and TE_x cases [Fig. 3(b)–(d)]. The TM RCS [Fig. 3(e)] again has its maximum at about 45° angle of incidence whereas the TE RCS is largest at broadside incidence ($\vartheta_{\mathrm{inc}} = 90°$) and is about an order of magnitude greater with respect to axial incidence ($\vartheta_{\mathrm{inc}} = 0°$), as in the case of the hollow layered dielectric cylinder.

The last example considered is the scattering from a lossy cylinder with a dielectric coating [Fig. 4(a)]. Five cases have been considered for the imaginary part ε_r'' of the relative permittivity of the cylinder, namely $\varepsilon_r'' = 0., 0.03, 0.3, 3., 30.$ The cylinder presents stronger directivity for the TM_x case [Fig. 4(b)–(d)] than the TE_x [Fig. 5(a)–(c)] case, whereas the TM_z illumination produces almost the same pattern as the TM_x case with respect to the propagation direction. The effect of the conductivity becomes evident for values of ε_r'' greater than 0.3 and results in reducing the scattered power, while

increasing both the forward and backward scattering. For low-loss values the behavior of the lossy cylinder on the incidence plane resembles that of the coated dielectric cylinder. These effects can also be seen in the RCS versus ϑ_{inc} plot [Figs. 4(e) and 5(d)].

IV. Conclusions

In this paper, a point-matching MoM scheme is presented which, for the case of scattering of an incident wave by a dielectric object, reduces the evaluation of the 3-D integrals of the interaction matrix elements to 2-D ones. The new relations for the interaction matrix elements maintain the same degree of approximation as the original ones and avoid the singularity of the DGF in the self dyad, thus making the application of MoM more flexible. Application is made and radiation patterns are given for scattering by various dielectric and lossy finite scatterers of cylindrical geometry illuminated by a uniform plane wave. The method can be extended to 2-D problems, thus reducing the surface integrals to line integrals.

References

[1] E. K. Miller, L. Medgyesi-Mitschang, and E. H. Newman, Eds., *Computational Electromagnetics*. Piscataway, NJ: IEEE Press, 1992.

[2] K. Umashankar, and A. Taflove, *Computational Electromagnetics*. Norwood, MA: Artech House, 1993.

[3] N. Morita, N. Kumagai, and J. R. Mautz, *Integral Equation Methods for Electromagnetics*. Norwood, MA: Artech House, 1990.

[4] A. Ishimaru, *Electromagnetic Wave Propagation, Radiation, and Scattering*. Englewood Cliffs, N.J.: Prentice-Hall, 1991.

[5] R. F. Harrington, *Field Computation by Moment Methods*. Piscataway, NJ: IEEE Press, 1993.

[6] M. M. Ney, "Method of moments as applied to electromagnetic problems," *IEEE Trans. Microwave Theory Tech.*, vol. MTT-33, pp. 972–980, Oct. 1985.

[7] C.-T. Tai, *Dyadic Green Functions in Electromagnetic Theory*, 2nd ed. Piscataway, NJ: IEEE Press, 1994.

[8] A. D. Yaghjian, "Electric dyadic Green's functions in the source region," *Proc. IEEE*, vol. 68, pp. 248–263, Feb. 1980.

[9] J. R. Mautz and R. F. Harrington, "Electromagnetic scattering from a homogeneous material body of revolution," *AEÜ* (Germany), vol. 33, pp. 71–80, Feb. 1979.

[10] P. Barber, and C. Yeh, "Scattering of electromagnetic waves by arbitrarily shaped dielectric bodies," *Appl. Opt.*, vol. 14, no. 12, pp. 2864–2872, Dec. 1975.

[11] K.-M. Chen, D. E. Livesay, and B. S. Guru, "Induced current in and scattered field from a finite cylinder with arbitrary conductivity and permittivity," *IEEE Trans. Antennas Propagat.*, vol. AP-24, pp. 330–336, May 1976.

[12] M. A. Morgan and K. K. Mei, "Finite-element computation of scattering by inhomogeneous penetrable bodies of revolution," *IEEE Trans. Antennas Propagat.*, vol. AP-27, pp. 202–214, Mar. 1979.

[13] L. E. Allan, and G. C. McCormick, "Measurements of the backscatter matrix of dielectric bodies," *IEEE Trans. Antennas Propagat.*, vol. AP-28, pp. 166–169, Mar. 1980.

[14] A. G. Papayiannakis, and E. E. Kriezis, "Scattering from a dielectric cylinder of finite length," *IEEE Trans. Antennas Propagat.*, vol. AP-31, pp. 725–731, Sept. 1983.

[15] D. H. Schaubert, D. R. Wilton, and A. W. Glisson, "A tetrahedral modeling method for electromagnetic scattering by arbitrarily shaped inhomogeneous dielectric bodies," *IEEE Trans. Antennas Propagat.*, vol. AP-32, pp. 77–85, Jan. 1984.

[16] D. H. Schaubert and P. M. Meaney, "Efficient computation of scattering by inhomogeneous dielectric bodies," *IEEE Trans. Antennas Propagat.*, vol. AP-34, pp. 587–592, Apr. 1986.

[17] K. Umashankar, A. Taflove, and S. M. Rao, "Electromagnetic scattering by arbitrary shaped three-dimensional homogeneous lossy dielectric objects," *IEEE Trans. Antennas Propagat.*, vol. AP-34, pp. 758–766, June 1986.

[18] S. S. Seker and A. Schneider, "Electromagnetic scattering from a dielectric cylinder of finite length," *IEEE Trans. Antennas Propagat.*, vol. 36, pp. 303–307, Feb. 1988.

[19] C.-C. Su, "Electromagnetic scattering by a dielectric body with arbitrary inhomogeneity and anisotropy," *IEEE Trans. Antennas Propagat.*, vol. 37, pp. 384–389, Mar. 1989.

[20] T. K. Sarkar, E. Arvas, and S. Ponnapalli, "Electromagnetic scattering from dielectric bodies," *IEEE Trans. Antennas Propagat.*, vol. 37, pp. 673–676, May 1989.

[21] R. A. Murphy, C. G. Christodoulou, and R. L. Phillips, "Electromagnetic scattering from a finite cylinder with complex permittivity," *J. Electromagnetic Waves and Appl.*, vol. 5, no. 9, pp. 983–996, Sept. 1991.

[22] S.-W. Lee, J. Boersma, C.-L. Law, and G. A. Deschamps, "Singularity in Green's function and its numerical evaluation," *IEEE Trans. Antennas Propagat.*, vol. AP-28, pp. 311–317, May 1980.

[23] D. R. Wilton, S. M. Rao, A. W. Glisson, D. H. Schaubert, O. M. Al-Bundak, and C. M. Butler, "Potential integrals for uniform and linear source distributions on polygonal and polyhedral domains," *IEEE Trans. Antennas Propagat.*, vol. AP-32, pp. 276–281, Mar. 1984.

[24] R. D. Graglia "The use of parametric elements in the moment method solution of static and dynamic volume integral equations," *IEEE Trans. Antennas Propagat.*, vol. 36, pp. 636–646, May 1988.

[25] R. D. Graglia, P. L. E. Uslenghi, and R. S. Zich, "Moment method with isoparametric elements for three-dimensional anisotropic scatterers," *Proc. IEEE*, vol. 77, pp. 750–760, May 1989.

[26] R. D. Graglia "On the numerical integration of the linear shape functions times the 3-D Green's function or its gradient on a plane triangle," *IEEE Trans. Antennas Propagat.*, vol. 41, pp. 1448–1455, Oct. 1993.

[27] J. R. Mautz, "Alternative derivation of the point-matching MoM reduced scheme to calculate scattering from a dielectric body," private communication, Mar. 1996.

Antonis G. Papagiannakis (S'76–M'77) was born in Thessaloniki, Greece, in 1954. He received the Diploma in electrical engineering and the Ph.D. degree from Aristotle University of Thessaloniki, Greece, in 1977 and 1986, respectively.

Since 1980, he has been working in the Electrical and Computer Engineering Department, Aristotle University of Thessaloniki, where he is currently an Assistant Professor. His areas of interest include electromagnetic wave propagation and scattering, optics, Green's functions methods, and numerical methods with emphasis on the MoM and beam propagation method.